Modeling and Simulation of Storm Surge on Staten Island to Understand Inundation Mitigation Strategies

Authors: Kress, Michael E., Benimoff, Alan I., Fritz, William J., Thatcher, Cindy A., Blanton, Brian O., et al.

Source: Journal of Coastal Research, 76(sp1) : 149-161

Published By: Coastal Education and Research Foundation

URL: https://doi.org/10.2112/SI76-013

Journal of Coastal Research	SI	76	149–161	Coconut Creek, Florida	2016

Modeling and Simulation of Storm Surge on Staten Island to Understand Inundation Mitigation Strategies

Michael E. Kress[†*], Alan I. Benimoff[†], William J. Fritz[†], Cindy A. Thatcher[‡], Brian O. Blanton[§], and Eugene Dzedzits[†]

[†]College of Staten Island, The City University of New York Staten Island, NY 10314, U.S.A.

[‡]U.S. Geological Survey Eastern Geographic Science Center Reston, VA 20192, U.S.A.

[§]Renaissance Computing Institute University of North Carolina at Chapel Hill Chapel Hill, NC 27517, U.S.A.

www.cerf-jcr.org

www.JCRonline.org

ABSTRACT

Kress, M.E.; Benimoff, A.I.; Fritz, W.J.; Thatcher, C.A.; Blanton, B.O., and Dzedzits, E., 2016. Modeling and simulation of storm surge on Staten Island to understand inundation mitigation strategies. *In*: Brock, J.C.; Gesch, D.B.; Parrish, C.E.; Rogers, J.N., and Wright, C.W. (eds.), *Advances in Topobathymetric Mapping, Models, and Applications*. *Journal of Coastal Research*, Special Issue, No. 76, pp. 149–161. Coconut Creek (Florida), ISSN 0749-0208.

Hurricane Sandy made landfall on October 29, 2012, near Brigantine, New Jersey, and had a transformative impact on Staten Island and the New York Metropolitan area. Of the 43 New York City fatalities, 23 occurred on Staten Island. The borough, with a population of approximately 500,000, experienced some of the most devastating impacts of the storm. Since Hurricane Sandy, protective dunes have been constructed on the southeast shore of Staten Island. ADCIRC+SWAN model simulations run on The City University of New York's Cray XE6M, housed at the College of Staten Island, using updated topographic data show that the coast of Staten Island is still susceptible to tidal surge similar to those generated by Hurricane Sandy. Sandy hindcast simulations of storm surges focusing on Staten Island are in good agreement with observed storm tide measurements. Model results calculated from fine-scaled and coarse-scaled computational grids demonstrate that finer grids better resolve small differences in the topography of critical hydraulic control structures, which affect storm surge inundation levels. The storm surge simulations, based on post-storm topography obtained from high-resolution lidar, provide much-needed information to understand Staten Island's changing vulnerability to storm surge inundation. The results of fine-scale storm surge simulations can be used to inform efforts to improve resiliency to future storms. For example, protective barriers contain planned gaps in the dunes to provide for beach access that may inadvertently increase the vulnerability of the area.

ADDITIONAL INDEX WORDS: *Lidar, ADCIRC, SWAN, dunes, flood protection, hard stabilization.*

INTRODUCTION

Hurricane Sandy, which made landfall on October 29, 2012, near Brigantine, New Jersey, had a significant impact on Staten Island and the New York Metropolitan area. Of the 43 fatalities resulting from Hurricane Sandy, 23 occurred in Staten Island, a borough of New York City that experienced some of the most devastating impacts of the storm.

There is confusion in both the scientific literature and the popular press as to whether the Sandy event should be referred to as Superstorm Sandy or Hurricane Sandy. Coch (2015) argues that while the surge generated by Hurricane Sandy was not a unique event, "The unique confluences of meteorological and astronomical factors in Sandy were very rare and unlikely to be repeated for a very long time." Because Sandy had hurricane force winds for much of its duration and gusts of hurricane force winds were briefly recorded in the New York Metropolitan area, here the event is referred to as Hurricane Sandy following the lead of Coch (2015). The important observation is that while Sandy was a rare meteorological event, tropical and extratropical storms similar to Sandy have occurred frequently since the 1600s, on average every 12 years (Benimoff, Fritz, and Kress, 2015).

Before Hurricane Sandy, the potential impacts of a large hurricane on Staten Island had been reported based on simulations (Benimoff *et al*., 2012) using the storm surge, tide, and wind-wave model ADCIRC (Luettich, Westerink, and Scheffner, 1992; Westerink *et al*., 2008) to model storm surge. To extend the conceptual model of Staten Island's vulnerability, new analyses are conducted for this study using the best track analysis for Hurricane Sandy to conduct hindcast simulations of water levels for comparison with observed storm tide measurements, and to assess impacts of current and potential engineered flood protection measures (Benimoff, Fritz, and Kress, 2015). By modifying ADCIRC's finite element grid to reflect alternative coastal protection concepts, the potential impacts of future storms can be simulated to model the effectiveness of various existing and proposed engineering structures and dune fields.

Given proposed flood protection design alternatives and the ongoing human modification to the coastal geomorphology, this study investigates impacts of these modifications on potential storm-induced flooding in the ocean-facing Staten Island area. The goals of this study are to (1) modify the unstructured grid used in ADCIRC to represent storm surge mitigation structures based on engineering designs, and quantify the effectiveness of

DOI: 10.2112/SI76-013 received 11 February 2015; accepted in revision 3 June 2015.

*Corresponding author: Michael.Kress@csi.cuny.edu

using high-resolution topographic data from lidar to better understand flood mitigation strategies; and (2) compare storm surge simulations based on engineering designs of mitigation structures to simulations based on "as built" structures.

The New York Metropolitan area is not usually considered a high risk area for hurricanes. However, Hurricane Sandy inflicted a devastating blow to the region. Severe storms (extratropical and tropical) in the New York Harbor area have been noted in historical records beginning in the 1600s. Based on tide gauge records at the Battery in Manhattan extending back to 1860, Brandon *et al*. (2014) report that the largest storm surge levels ever observed there are due to Hurricane Sandy.

Brandon *et al.* (2014) used sediment cores to construct an inundation record covering the past ~300 years, determining that extreme flood events have occurred before in the New York Harbor area (including a major hurricane in 1821) and that the return interval for flood events similar to Hurricane Sandy is probably shorter than current estimates based on tide records alone. However, historical storms generally had little economic impact, at least on Staten Island, because the surges flowed across undeveloped marshland (Benimoff, Fritz, and Kress, 2015). With the rapid urbanization and population expansion that has occurred along the ocean-facing coast of Staten Island over the past 50 to 100 years, the economic and human vulnerability of this region to storms has greatly increased.

A review of past Atlantic hurricane tracks (Elsener and Kara, 1999; Scileppi and Donnelly, 2007) shows that many Atlantic hurricanes originate off the west coast of Africa and travel west, with some veering northward up the east coast of the United States. If the storms travel sufficiently far northward, as did Hurricanes Irene (2011) and Sandy (2012), the New York Metropolitan area is particularly vulnerable. Hurricane Sandy was a "coast normal" hurricane, making an almost perpendicular landfall on the New Jersey coast. The recurring interval of the track of Hurricane Sandy has been estimated at about 714 years, making the track, but not necessarily the storm surge, a rare event (Hall and Sobel, 2013). The track angle and landfall location put the northeastern quadrant of the hurricane in the New York Metropolitan area, where the storm's forward speed and cyclonic surface wind speed are additive, usually producing the greatest storm surge. In addition, the coast in the New York Metropolitan area forms a right angle, where Raritan Bay meets the New Jersey Shore to the south and meets Long Island to the north (Coch, 1999, 2012, 2014, 2015; Figure 1). This juncture acts effectively as a funnel, forcing the surge into Raritan Bay and flooding the coastline of Staten Island. Storm surges typically move northward into New York Harbor and meet the water being forced westward from Long Island Sound south into the East River. Staten Island is particularly vulnerable in this regard, as it is located at the confluence of the Hudson River, Lower Bay, and Raritan Bay.

Generally larger storm tides combined with a 0.44-m increase in local sea level since 1856 have led to an increased probability of extreme flood events (Talke, Orton, and Jay, 2014). An analysis of long-term relative mean sea level trends on the mid-Atlantic coast indicates that observed increases in mean sea level from 1950–2012 and variability in ocean circulation patterns have contributed to a one- to two-thirds decrease in the recurrence interval of inundation events similar to Hurricane Sandy (Sweet *et al*., 2013).

There are several dynamic models typically used to model storm surge. These models range from the National Oceanic and Atmospheric Administration's (NOAA) Sea Lakes and Overland Surges from Hurricanes (SLOSH) (Jelesnianski, Chen, and Shaffer, 1992), which runs on one CPU but sacrifices spatial resolution and some physics for the sake of this efficiency to spatially detailed, high-resolution models like ADCIRC (Luettich, Westerink, and Scheffner, 1992; Westerink *et al.*, 2008) and FVCOM (Qi *et al.*, 2009), which are formulated with either finite elements or finite volumes. These unstructured or non-rectangular implementations permit very high spatial resolution in regions of interest (like coastal areas threatened by storm-driven inundation) without unneeded resolution elsewhere (offshore, for example). The cost of this flexibility, however, is that relatively larger computer resources are needed to conduct simulations. The high-resolution capability can explicitly represent features that control the conveyance of storm-driven water. Other models include SELFE (Zhang and Baptista, 2008) and sECOM (Blumberg and Georgas, 2008).

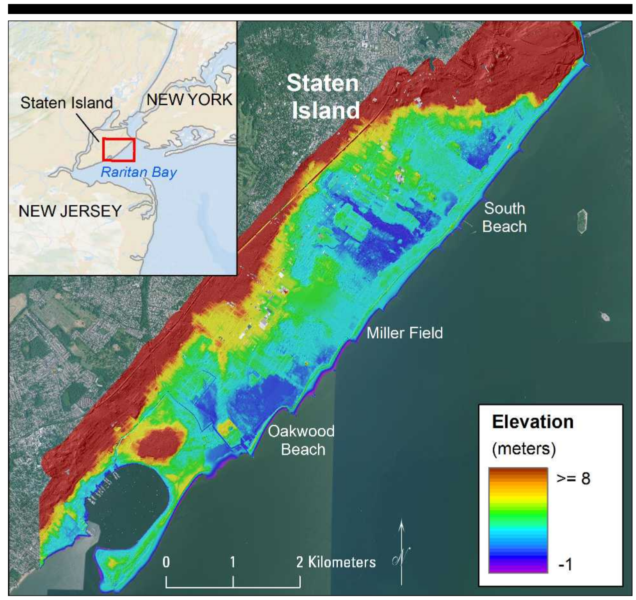

Figure 1. Map of the study area showing the elevation of the south coast of Staten Island. In the inset map, the right angle in the coastline where Long Island and the coast of New Jersey meet is visible.

Several recent pre-Sandy studies have quantified the threat to the New York–New Jersey (NY/NJ) area from storm-driven surge. Colle *et al.* (2008) provide an excellent overview of the New York Metropolitan area's vulnerability to storm surge and show how sensitive storm surge solutions are to changes in storm characteristics, particularly for tropical systems that are transitioning toward extratropical as they progress poleward. Lin *et al.* (2010) used both ADCIRC and SLOSH to conduct a probabilistic risk assessment for the area with large numbers of synthetic hurricanes to compute recurrence intervals for storm surge levels. Orton *et al.* (2012) used sECOM to study impacts of Hurricane Irene (2011) on the New York City region, performing a series of numerical experiments that partition the source contributions (*e.g.*, remote meteorological forcing, atmospheric pressure gradient, and freshwater inputs via rivers) into their impacts on storm surge predictions. Bowman *et al.* (2013) review model applications for the region and focus on potential interactions between storm surge and rising sea levels.

There have been several important numerical studies of Hurricane Sandy impacts in the NY/NJ region using several different models. Forbes *et al.* (2014) conducted simulations using the SLOSH storm surge model to assess the storm surge forecast skill of this relatively coarse resolution, rectangular grid model. Wang *et al*. (2014) used a sub-model approach, combining recent lidar and detailed urban infrastructure with the SELFE model (Zhang and Baptista, 2008) to hindcast inundation during Hurricane Sandy. However, Staten Island and its vulnerability to extreme coastal storms has yet to be directly addressed and is an understudied area, given the population density of an entire borough of New York City with nearly a half-million residents.

Since the occurrence of Hurricane Sandy, the U.S. Geological Survey (USGS) has conducted extensive fieldwork in the impacted area to provide quantitative assessments of high-water marks and elevations. Several groups coordinated by the USGS have gathered a comprehensive set of observations of high-water marks and extents of inland inundation. Using these data, as well as high-resolution post-storm elevation measurements obtained along the south shore of Staten Island, existing ADCIRC grids were modified to evaluate the current vulnerability of Staten Island to future storms and to model the potential impacts of built stabilization structures (Pilkey *et al.*, 2011) on the Staten Island coastline.

The New York City Department of Parks and Recreation (NYCDPR) installed in late 2013 a 3.96-m-high (NAVD88) artificial dune on Staten Island along the south shore from South Beach to Oakwood Beach, but excluding the Miller Field unit of Gateway National Recreation Area. The dune is composed of sand reinforced with 1.52-m-high by 4.57-m-wide geotextile trap bags. The NYCDPR artificial dune does not continue along the beach in front of Miller Field because that land is managed by the National Park Service (NPS), which maintains a natural dune at Miller Field. The NPS initiatives to protect the coastline include conducting coastal monitoring over many years and continuing a longstanding approach to cultivating the natural accretion and stability of the dune. For example, vegetation was planted on the dunes to replenish the natural vegetation ecosystem to inhibit sand erosion and increase sand volume due to washover. During Hurricane Sandy, the extensive root system likely slowed the flow of water and held most of the sand in place, providing greater stability and flood mitigation to the Miller Field site than an un-vegetated dune.

Using numerical storm surge and wave models, the water level response to Hurricane Sandy was computed for a sequence of different coastal land configurations. This paper describes the computational methods and model grids, and compares storm surge simulations based on designed mitigation structures versus "as built" structures. The technical goals of this study are to understand the benefits and costs of incorporating high-resolution terrain mapping data into the numerical grids used in ADCIRC for studying flooding due to storm surges on Staten Island.

METHODS

This study combines high-resolution numerical simulations, USGS observations of high-water marks, and post-storm airborne lidar (light detection and ranging), terrestrial lidar, and Global Positioning System (GPS) surveys to assess the impacts of pre- and post-Sandy dune elevations and possible protective measures for Staten Island. The finite element storm surge, tide, and wind-wave modeling software ADCIRC (Luettich, Westerink, and Scheffner, 1992; Westerink *et al.*, 2008) is used in its vertically integrated formulation. Research and applications with ADCIRC cover a range of coastal oceanographic and engineering problems, including regional and local tidal phenomena (Westerink, Luettich, and Muccino, 1994; Blanton *et al.*, 2004), coastal wetlands restoration impacts (Wamsley *et al.*, 2010), coupled storm surge and wave hindcasts (Atkinson, Westerink, and Hervouet, 2004; Dietrich *et al.*, 2011), and real-time forecasting of storm surge and wind-waves (Blanton *et al.*, 2012; Fleming *et al.*, 2008). ADCIRC is approved by the Federal Emergency Management Agency (FEMA) for computing storm surge flood hazard simulations and continues to be used for the development of Digital Flood Insurance Rate Maps (DFIRMs) in Texas, Louisiana, Mississippi, Alabama, Delaware, Virginia, North Carolina, South Carolina, Georgia, and Florida (*e.g.*, Blanton, 2008; Niedoroda *et al.*, 2010). ADCIRC has recently been formally coupled to the wind-wave model Simulating Waves Nearshore (SWAN) (Booij, Ris, and Holtuijsen, 1999) by recasting SWAN into finite element form (Dietrich *et al.*, 2011; Zijlema, 2010). The coupled nature of ADCIRC+SWAN does not require interpolation of data fields between ADCIRC and SWAN, thus substantially simplifying the data file management. ADCIRC provides winds and water levels to SWAN, and SWAN computes radiation stress gradients directly on the finite element triangular grid and provides these to ADCIRC.

The triangular, finite element spatial discretization used in ADCIRC allows for flexible resolution. Nodes are generally placed at higher density in coastal regions of interest, with relatively coarser resolution in deep water. When simulating coastal flooding and inundation, the grid extends sufficiently far inland to avoid artificial blockage of water against the landward boundary. The very large ocean domain set-up captures ocean waves that propagate from offshore into the shallower coastal areas. Figure 2a shows the computational domain used in ADCIRC. The only open boundary is positioned at the 60-degrees west meridian. Figure 2b shows the computational grid in the Staten Island area.

ADCIRC solves for the water level and currents driven by tides, atmospheric winds and pressure, and wave radiation stress

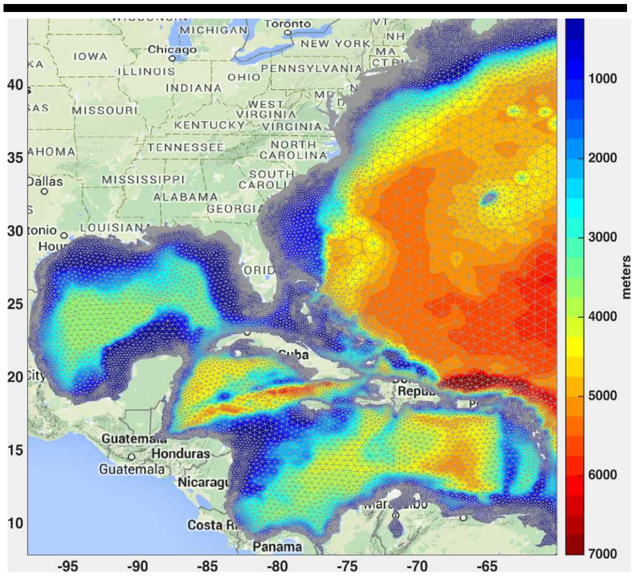

Figure 2a. The computation domain of the ADCIRC model showing the FEMA Region II coarse grid. The colors represent the bathymetry and elevation.

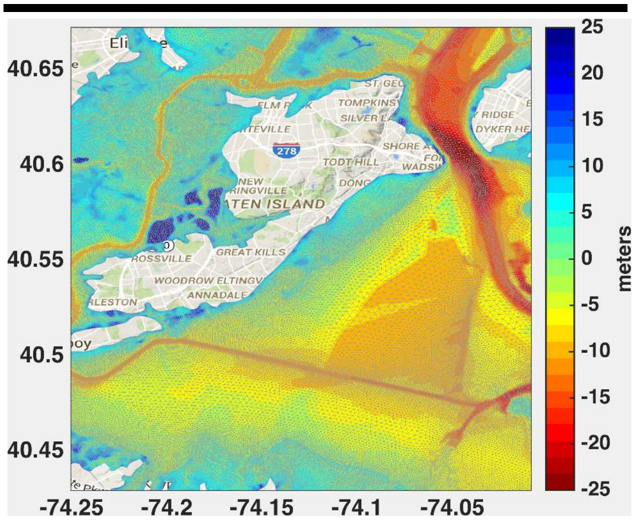

Figure 2b. The computational grid in the Staten Island, NY, study area. The colors represent the bathymetry and elevation, ranging from –25 m in the channels to 25 m inland.

gradients as computed by the SWAN model. Boundary conditions for the tidal elevations were extracted from the most recent OTIS Regional Tidal Solutions for the North Atlantic Ocean (Egbert and Erofeeva, 2002) and applied to the open boundary. The constituents used are M2, N2, S2, K2, K1, O1, P1, and Q1 (Table 1). The same constituents are used for tidal potential forcing.

The ADCIRC grids used (described further below) have minimum resolutions of about 20 and 70 m. The model time step is thus relatively small at 0.5 s. For SWAN, the default Komen white capping (Vledder, Zijlema, and Holthuijsen, 2011) and JONSWAP bottom friction was used with a coefficient of 0.038 (Bouws and Komen, 1983). The SWAN time step is 900 s, meaning that ADCIRC and SWAN exchange information every 1,800 ADCIRC time steps.

ADCIRC's quadratic bottom friction is used with a Manning's *n* approach for determining the drag coefficient. Spatially variable Manning's *n* is determined from land cover datasets and classifications developed by the USGS and available in the National Land Cover Database (NLCD) (Jin *et al*., 2013). The determination of the Manning's *n* coefficients is described in Bunya *et al.* (2010). Wind stress modifications are made through a directionally dependent roughness length and a tree canopy effect, both of which are derived from the NLCD land cover datasets.

Meteorological forcing for simulating Hurricane Sandy is derived from NOAA's best track analysis database (NOAA, 2013). Best track information includes storm central pressure, storm center location, and radius to the standard wind speeds of 34, 50, and 64 knots in the four storm quadrants. This information is used in ADCIRC's internal vortex wind model (Mattocks and Forbes, 2008) to compute time-dependent ten-m wind and sea level pressure fields.

While this is not a detailed study of the wind fields associated with Hurricane Sandy, it is important that the wind field used reasonably represents actual storm conditions, at least in the vicinity of the NY/NJ area. Since the simulation uses a parametric vortex representation of the hurricane, with parameters taken from the best track analysis, the true wind and pressure fields far away from the storm center will not be well represented by the vortex assumption. This is particularly true with a hurricane that has merged with larger continental systems.

The starting date in the best track is October 23, 2012. The storm's track is shown in Figure 3a, along with a snapshot of the vortex wind field at October 29, 2012, 20:00 UTC (Figure 3b). Each Sandy simulation was preceded by a 52-day-long spin-up period starting September 1, 2012, where the tides were ramped up gradually over 10 days and allowed to stabilize before starting the meteorological component of the simulations. Figure 4 shows the wind speed (Figure 4a) and sea level atmospheric pressure (Figure 4b) at the NOAA Coastal Marine Automated Network (C-MAN) station 44056, located at about 25 m depth in New York Harbor, about 28 km southeast of Breezy Point (location shown in Figure 1). The peak wind speeds in ADCIRC reach about 25 m/s, while the observed wind speed is slightly less at 24 m/s. Also, the observed winds have much higher variability due to the hourly availability of C-MAN observations than the best track locations that are specified at 6 hourly intervals. The atmospheric pressure reaches a minimum of 962 mb and 958 mb for the ADCIRC and observed C-MAN data, respectively.

Table 1. *Tidal constituents used for open boundary and tidal potential forcing. Nodal factors and equilibrium arguments are for the start date of September 1, 2012.*

Constituent Name	Description	Period [hrs]	Frequency [rad/s]	Tidal Potential Amplitude [m]	Earth Elasticity Factor	Nodal Factor	Equilibrium Argument [deg]
M_2	Principal lunar	12.42	0.000141	0.242334	0.693	1.02	5.1
N_2	Larger lunar elliptic	12.66	0.000138	0.046398	0.693	1	0
S_2	Principal solar	12	0.000145	0.112841	0.693	1.02	264.9
K_2	Larger lunar elliptic	11.97	0.000146	0.030704	0.693	0.87	336.9
K_1	Lunisolar semidiurnal	23.93	7.29E-05	0.141565	0.736	0.87	336.9
O_1	Lunisolar diurnal	25.82	6.76E-05	0.100514	0.695	0.92	102.3
P_1	Principal solar diurnal	24.07	7.25E-05	0.046843	0.706	1	109.44

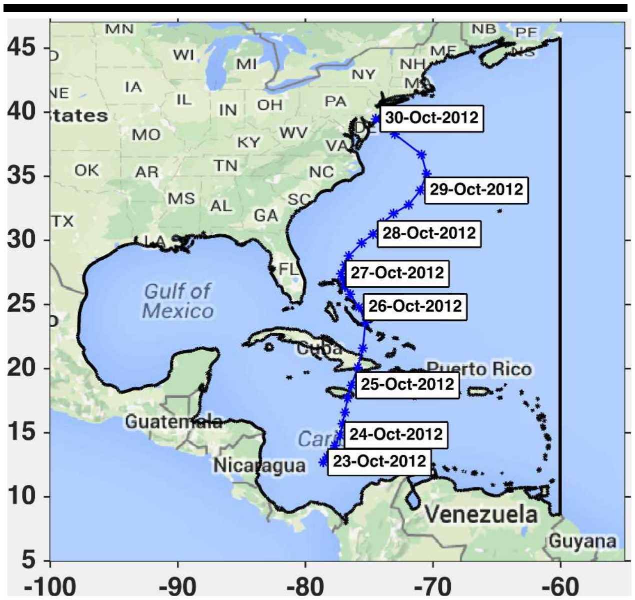

Figure 3a. Hurricane Sandy storm track from the NOAA best-track analysis.

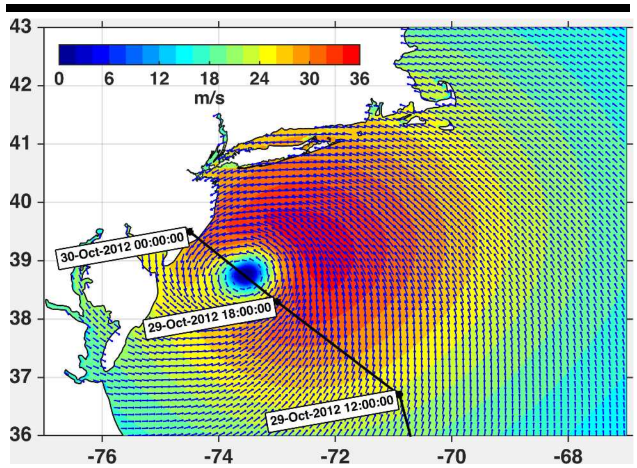

Figure 3b. Snapshot of the ADCIRC vortex wind field for Hurricane Sandy at October 29, 2012, 20:00 UTC. The wind speed is in m/s and the vectors show the wind direction.

Computational Grids

ADCIRC's finite element formulation permits localized high resolution in the areas with features that control hydraulics and hydrodynamics, including creeks, estuaries, channels, and overland features such as sand dunes, raised roadways, and levees, without unnecessary resolution in the continental shelf and deep-ocean areas. Software used for defining the grid node topographic elevations and bathymetric depth included Matlab (The MathWorks, Inc., Natick, MA), ArcGIS (Esri, Redlands, CA), Arc StormSurge (Ferreira, Olivera, and Irish, 2014), and the Surface Water Modeling System (SMS; Aquaveo, Provo, Utah).

The baseline ADCIRC grid was developed for the recent FEMA Region II coastal flood insurance study. This "coarse" grid has 604,790 nodes and includes the U.S. Atlantic coast, the Gulf of Mexico, and the Caribbean Sea (Figure 2a). Coastal resolution in the New York Harbor area ranges from 70 m to

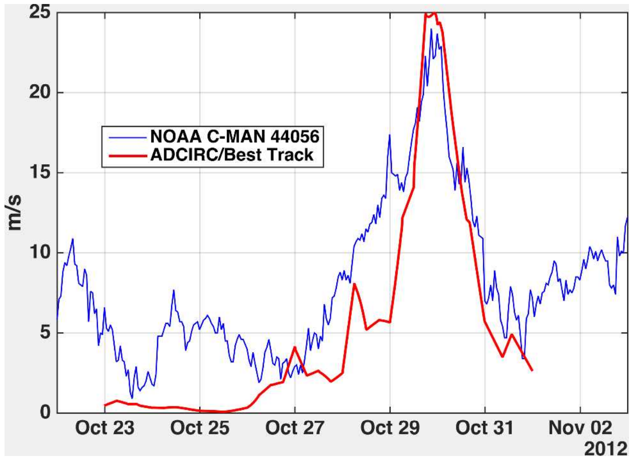

Figure 4a. Time series of observed (blue) and ADCIRC vortex (red) wind speed.

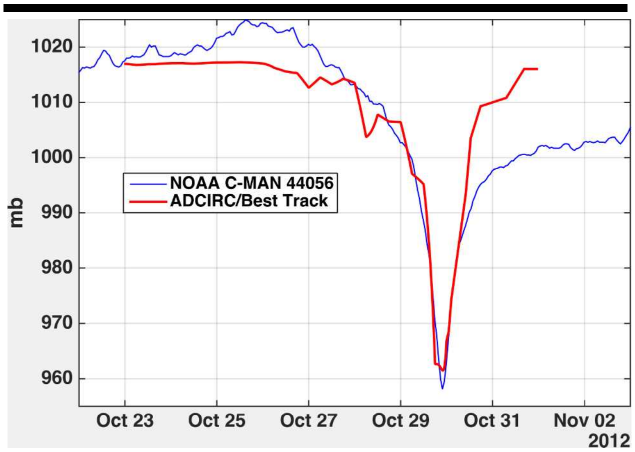

Figure 4b. Sea level pressure at the NOAA C-MAN 44056 station in New York Harbor.

400 m (Figure 2b). Along the southeast coastline where the high-resolution digital elevation model (DEM) was used, the grid spacing varies from approximately 70 m to approximately 150 m (Figure 5a). The grid spacing generally varies by location based on the gradient of the elevation with the smallest grid spacing near the shoreline and gradually increasing farther inland. This grid was used with ADCIRC+SWAN to compute statistical water levels for developing FEMA Region II Digital Flood Insurance Rate Maps (D-FIRMs), which were released in December 2013.

A higher resolution "fine" grid with 801,356 nodes was also used for comparing the impacts of additional spatial resolution on the computed storm surge. This grid, provided by the

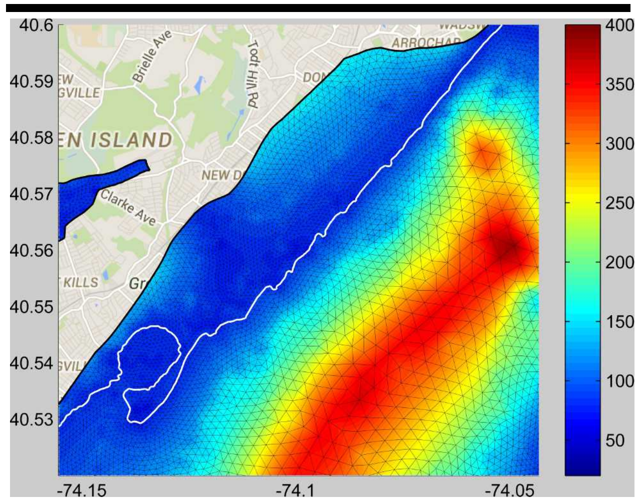

Figure 5a. An image of the finite element coarse computational grid shaded with grid spacing, ranging from 20 m (blue) to 400 m (red).

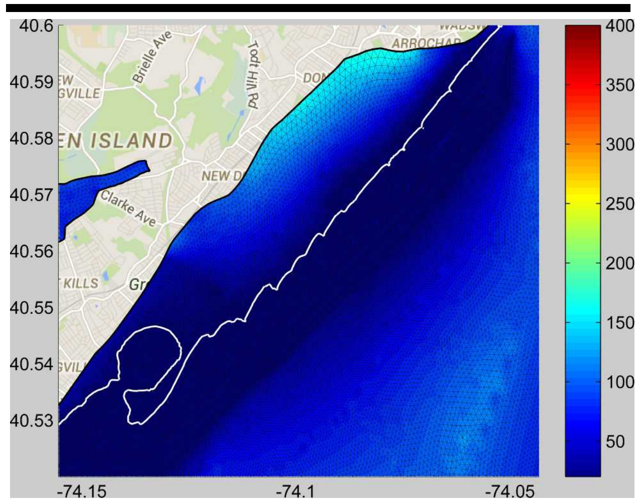

Figure 5b. An image of the finite element fine computational grid shaded with grid spacing, ranging from 20 m (blue) to 400 m (red).

ARCADIS engineering firm (ARCADIS U.S., Inc., Highlands Ranch, CO), was used for flood mitigation engineering and design studies in the region. The grid spacing in the Staten Island study area ranges from approximately 20 m near the shoreline to 200 m in channels in Raritan Bay. On the southeast coastline where the high-resolution DEM was used, the fine grid spacing varies from approximately 20 m to approximately 70 m (Figure 5b). The topography and bathymetry for both the coarse and fine grids are based on pre-Sandy conditions.

Post-Sandy Elevation Surveys

The potential impacts of a future extreme storm on the present (post-Sandy) geomorphology of the Staten Island coast were examined by modifying the topography and bathymetry of the coarse and fine grids to reflect post-Sandy conditions. The post-Sandy elevation data represent coastal morphological changes from erosion, overwash, and inundation, as well as human-induced changes including the construction of artificial dunes and other shoreline protection structures.

The data include 2012 post-Sandy airborne lidar obtained from the U.S. Army Corps of Engineers (USACE). These airborne topographic and bathymetric lidar data were collected on November 16, 2012, using the USACE Joint Airborne Lidar Bathymetry Technical Center of eXpertise (JALBTCX) Coastal Zone Mapping and Imaging Lidar (CZMIL) system (USACE, 2012), with a nominal point spacing of 1 m. In addition, the USGS collected field survey data in April 2014 using real-time kinematic (RTK) GPS and terrestrial lidar. The field survey covered the coast of Staten Island from the south end of the Great Kills unit of Gateway National Recreation Area to the northern end of the Franklin D. Roosevelt Boardwalk. The GPS points were collected using shore normal transects spaced at 50–100-m intervals, with 10–20-m within-transect spacing, depending upon the complexity of the topography. High-density terrestrial lidar data were collected along the artificial dunes parallel to the Midland Beach promenade. The terrestrial lidar and RTK GPS data were interpolated into a 1-m resolution DEM using a kernel interpolation with barriers algorithm in ArcGIS. The USACE post-Sandy lidar data are the source of the elevation data in the DEM for parts of the ocean-facing coast of Staten Island that were not surveyed with GPS.

To simulate the impacts of a Sandy-like storm on the current geomorphic structure of the coastline, a direct lookup method was used to assign the elevation of the nodes based on the DEM. While other methods such as a cell averaged technique (Bilskie and Hagen, 2013) may provide better results in areas with irregular or highly vegetated coastlines, the direct lookup method is expected to provide good results for the 20-m and 70-m resolution grids in terms of the impacts of resolution on computed storm surge.

RESULTS

The model simulations were run using grids with pre–Hurricane Sandy elevations and compared to measured high-water marks reported for the storm by the USGS (McCallum *et al*., 2012) at 16 locations on Staten Island. The observed and simulated maximum water levels for both coarse and fine grids are shown in Table 2. The observation locations are shown in Figure 6 along with the maximum water elevation for the pre-Sandy fine grid simulation. There are a few locations at which the modeled water level was dry. For these, the nearest wet node was used for comparison, indicated by an asterisk (*) in Table 2. In these cases, the grid did not adequately represent irregularities in the shoreline. For instance, point D represents a high area at Great Kills Park so the nearest wet node was used, which was two nodes away for the coarse grid and four nodes away for the fine grid. At locations A, F, I, K, and N there were small cliffs, and the nearest wet nodes were one grid point away. Similar comparisons between simulations and USGS high-water marks appear in Simonson and Behrins (2015) and Forbes *et al.* (2014).

Table 2. *Comparison of high-water marks with simulations.*

ID	Longitude	Latitude	Recorded High-Water Mark (m)	Coarse Grid Pre-Sandy Max Water Level (m)	Fine Grid Pre-Sandy Max Water Level (m)
A	-74.0683	40.5938	3.87	3.59*	3.63*
B	-74.0985	40.5822	3.81	3.71	3.77
C	-74.1166	40.5552	3.81	3.7	3.77
D	-74.1238	40.5458	4.27	3.64*	3.92*
E	-74.1437	40.5393	2.99	3.66	3.75
F	-74.1588	40.5284	5.15	3.77*	3.84
G	-74.1944	40.5154	3.96	3.89	3.93
H	-74.2104	40.5115	3.99	3.8	3.94
I	-74.2312	40.5023	4.02	3.84*	3.95
J	-74.2412	40.4997	4.02	3.91	4.02
K	-74.2538	40.5024	3.99	3.89*	3.99*
L	-74.1663	40.5924	3.75	3.45	3.64
M	-74.1359	40.6412	3.51	3.34	3.44
N	-74.0896	40.6468	3.57	3.41*	3.47*
O	-74.0739	40.6377	3.57	3.45	3.51
P	-74.0631	40.6156	4.66	3.4	3.48
	RMSE			0.54	0.49

The fine grid results are slightly better than those for the coarse grid as far as inundation extent, showing inundation values for the maximum water elevation at 12 of the 16 high-water mark locations, while the coarse results showed water at 11 of the 16 locations. For the fine grid, nine of the locations showed agreement of less than 7 cm from the observed results. The root mean squared error (RMSE) was 49 cm. The coarse grid differences from the measured high-water marks were approximately twice the fine grid differences but still quite acceptable with an RMSE of 54 cm.

Simulations were run using both coarse and fine grids with pre-Sandy and post-Sandy elevation data. In addition, two simulations were run with elevations along the southeast coastline based on the design of the NYCDPR dune system. These "as designed" simulations use coarse pre-Sandy grids that were adapted to include a reconstructed dune system along the Staten Island shoreline. These simulations indicated that the "as designed" dune structure could provide significant protection to the Staten Island coastal areas from a Sandy-like storm.

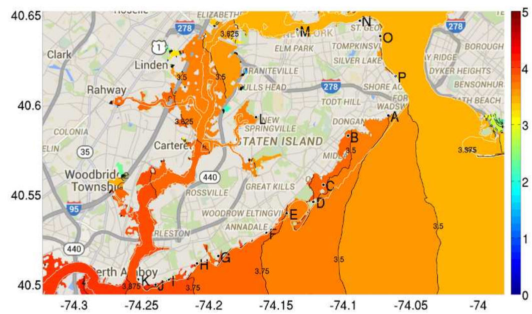

Figure 6. The maximum water elevation in m on Staten Island from the Hurricane Sandy hindcast simulation using pre-Sandy elevation data. The letters A–P are the location where high-water marks reported by USGS are compared to simulation results.

Figure 7a shows the simulation results for a Sandy-like storm in the study area for the pre-Sandy fine grid, and Figure 8a shows the results for the corresponding pre-Sandy coarse grid. Figure 7b presents the model results with the assumption of a continuous dune, based on the NYCDPR engineering design. Figure 7c shows the results with the dune along the southeast coast, except in the area of Miller Field where pre-Sandy elevations were used. Finally, Figure 7d presents the fine grid results with post-Sandy elevations from the November 2012 airborne lidar surveys and April 2014 field surveys.

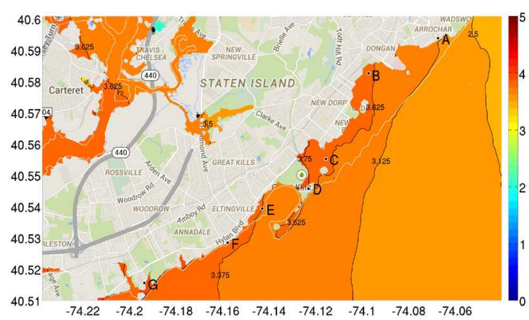

Figures 7a–7d. The maximum water elevation for Hurricane Sandy hindcast simulations for four different coastline configurations. The white line indicates the zero elevation contour. Figure 7a shows the pre-Sandy fine grid results.

Post-Sandy simulations were run using both the coarse grid and the higher resolution fine grid. The results of the fine grid simulation are shown in Figure 7d and the coarse grid simulation in Figure 8b. Interestingly, Figure 8b shows larger gaps and more extensive flooding of the coastal areas than the fine grid simulations. This is an artifact of the relatively coarse grid size of 70–80 m. The fine grid, with its 20-m resolution, shows less flooding and enables us to more accurately pinpoint gaps in the dune structure.

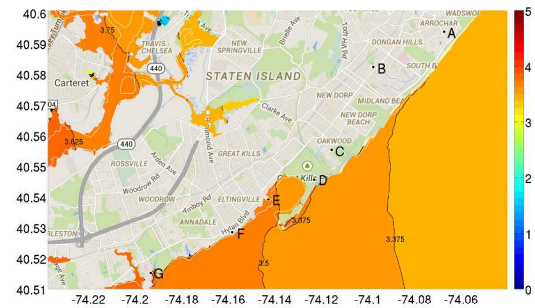

Figure 7b represents the model with the assumption of a continuous sand dune based on the NYCDPR design.

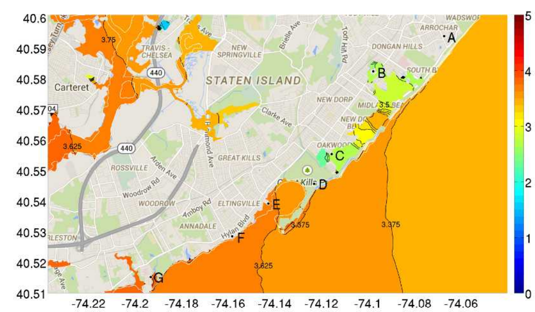

Figure 7c represents a discontinuous sand dune configuration comprised of the natural sand dune along the Miller Field shoreline and the “as designed” NYCDPR sand dune from Great Kills to South Beach.

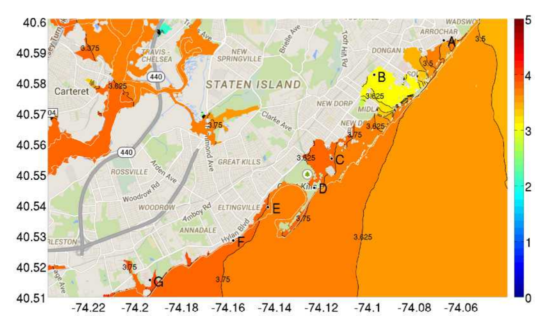

Figure 7d shows the model with the “as built” elevations based on the post-Sandy elevation data.

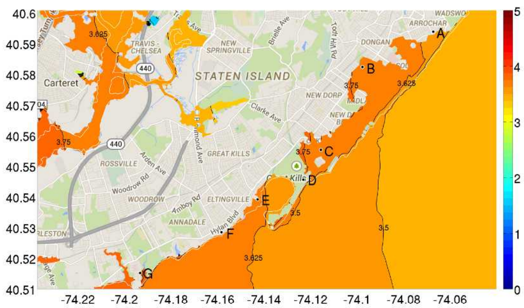

Figure 8a–8b. Maps of the maximum water elevation for the simulated Hurricane Sandy hindcast coarse grid models. The white line is the zero elevation contour. Figure 8a shows the results modeled with the pre-Sandy topography.

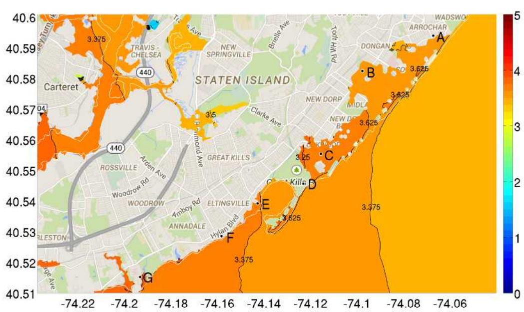

Figure 8b shows the maximum water elevations based on post-Sandy topography.

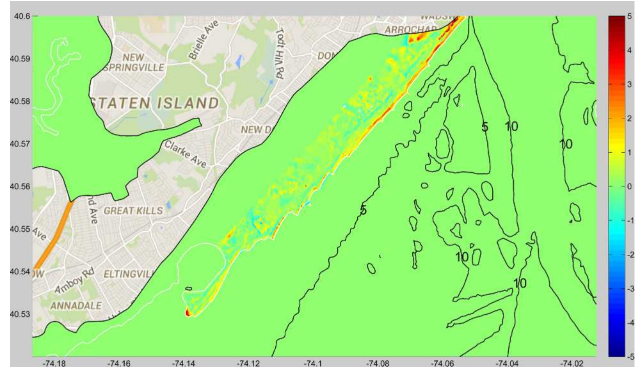

Figure 9a. An image of the difference in elevation in m between the pre- and post-Sandy fine grids. The locations in the red and yellow show the increase in elevation due to the construction of the NYCDPR dune.

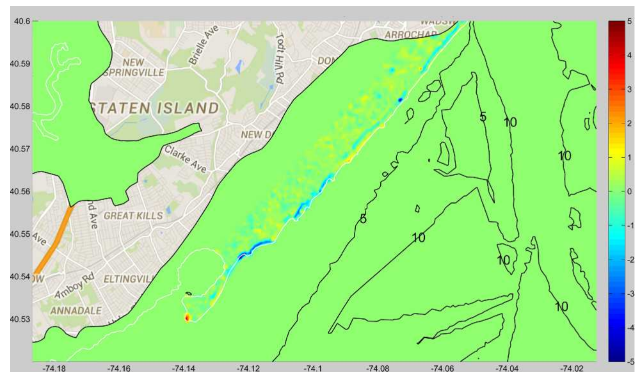

Figure 9b. An image of the elevation difference between the "as designed" grid and the post-Sandy "as built" grid along the southeast coastline where the high-resolution DEM was used for the post-Sandy "as built" grid.

The difference in elevation from pre-Sandy to post-Sandy for the fine grid model is shown in Figure 9a. The locations in red and yellow show increases in elevation from the pre-storm to post-storm conditions, and blue shows a decrease in elevation. Similarly for the coarse grid, Figure 9b shows the difference in elevation based on the design of the NYCDPR dune and the "as built" post-Sandy elevation. The locations in red and yellow show increases in the elevation from the pre-storm to post-storm conditions, and blue shows a decrease in elevation.

To better evaluate the impact of grid resolution on the storm surge results, Figure 10 shows a comparison of coarse to fine grid results. Figure 10a shows that pre-Sandy results are similar except in the fringes of the grid, shown in blue, where the resolution of the coarse grid was not sufficient to make a direct comparison between the two results. Also, in the Miller Field area, the coarse grid spacing was too large to represent the natural dune. As a result, the dune was not adequately resolved.

In the post-Sandy results shown in Figure 10b, which incorporates the high-resolution elevation measurements, the water levels are much higher in the coarse-scale model results than the fine-scale model. Red areas show that the coarse grid did not use the elevation data as effectively as the fine grid simulations. The coarse grid simulations resulted in overtopping and flooding in the low-lying areas behind the dunes, whereas the fine-scale simulations indicated that the dune system provides some additional protection from flooding.

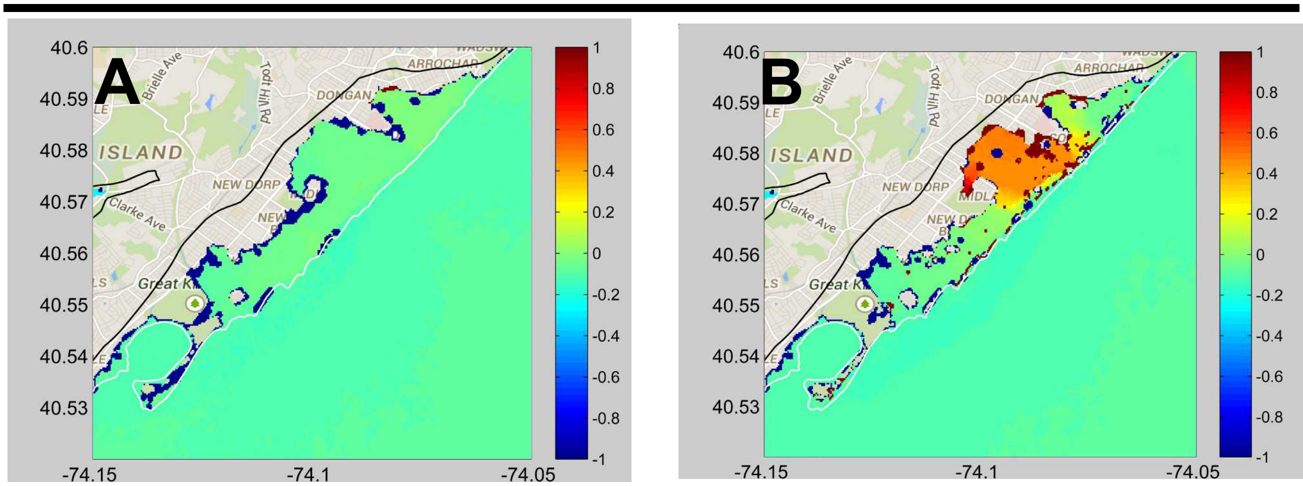

Figure 10. A comparison of the coarse grid results to the fine grid results, in m. The maximum water elevations for the coarse grid models minus the fine grid maximum water elevations are shown. The color ranges from blue, where the fine grid inundation is higher, to red, where the coarse grid inundation is higher. The white line indicates the zero elevation contour. (A) Pre-Sandy comparison. (B) Post-Sandy comparison.

DISCUSSION

The post-Sandy simulations show that the Staten Island coast is still susceptible to flooding, despite the reconstructed dunes. The availability of the post-Sandy elevation data enabled us to run simulations using the elevation survey data on the "as built" dunes instead of the engineering data for the "as designed" dunes. It also allowed us to identify locations of gaps in the 3.96-m-high dune. The artificial dunes constructed by NYCDPR and the natural, vegetated dunes adjacent to Miller Field with elevations between 3.5 m and 4 m in sections are discontinuous because of differences in management practices and the presence of a road and jetty at the property boundary at New Dorp Lane. This area warrants further study and a more comprehensive elevation survey. Planned gaps in the dunes to provide for beach access may inadvertently increase the vulnerability of the area.

The density of unstructured grid nodes is highest around the land-water interface in order to accurately represent significant topographic features that can alter the flow of water across the landscape. In addition, the computational grids are oriented along the coastline as are the dunes. While other methods such as a cell averaging technique (Bilskie and Hagen, 2013) exist to assign elevation values to grid nodes and may provide better results, a direct lookup method was used in this study because the density of nodes within the fine-scale grid is high enough to adequately represent key topographic features such as dunes, roads, and low-lying wetlands near the coastline. For the coarse-scale grid, the density of nodes was much lower and was unable to capture the topographic variation along the coastline regardless of the type of resampling method used.

Lidar-based DEMs, with very fine vertical and horizontal resolution, and current computing technology, can economically support even finer-level analyses. In addition, GPS and terrestrial lidar surveys could provide cost-effective, frequent and rapid updates on the topography of critical areas in flood zones. The significant cost elements are computer software, lidar data acquisition, and creating the unstructured grid, rather than incorporating updated elevation data or running simulations. Furthermore, the impacts of increases in sea level and projected increases in the ferocity of storms may encourage the use of finer-scale models and more frequent and larger simulations. Once the ADCIRC models and unstructured grids have been developed, the simulations can be updated and run on a periodic basis for a relatively low cost so that managers can respond to changing coastal conditions.

The consideration of erosion due to wave action or overwash is beyond the scope of this study. Therefore, potential mitigating impacts of the wide natural dune at Miller Field are not evident. A future study of the effects of erosion and mass transport with an appropriate model such as XBeach (Roelvink *et al.*, 2009) would provide better understanding of advantages, flood protection, and vulnerabilities of the Miller Field dune system.

Computer Resources and Timing

Simulations were conducted on the Cray XE6M housed in The City University of New York Interdisciplinary High-Performance Computing Center (CUNY-IHPCC) located at and operated by the College of Staten Island. This system was also used by ARCADIS and the Stevens Institute of Technology for modeling the potential impact of future hurricanes and sea level rise caused by climate change as a part of the City of New York's Special Initiative for Rebuilding and Resiliency and reported in PlaNYC (2013).

The XE6M supports the partitioned global address space programming model and has 176 shared memory computational nodes with each node having 16 cores, for a total of 2,816 computational cores. The machine has a theoretical peak performance of 25.3 teraFLOPS. The cores operate at 2.3 GHz with four floating-point operations per clock cycle. The nodes are tightly coupled with an interconnection network that supports advanced synchronization and communications features such as globally addressable memory and atomic memory operations, and fast message passing interface (MPI) traffic, as well as a fast input/output (I/O) to a global, shared file system. The interconnection network is based on a 2D torus topology that combines HyperTransport3 and proprietary protocols. The Cray Gemini chip on each node functions as the router chip and supports global memory addressability. The system also has a 126-terabyte parallel file system.

For the study simulations, ADCIRC+SWAN ran on 256 cores at an ADCIRC time step of 0.5 s. On the XE6M, simulations took 19.42 h and 14.37 h of wall time for the fine and coarse grids, respectively. Table 3 shows The CPU time for the spin-up and the Sandy simulation for both grids.

Table 7. *CPU Time for Hurricane Sandy simulations.*

	Coarse Grid	Fine Grid
Spin-up	8.87 h	11.94 h
Hurricane Sandy	5.5 h	7.48 h
Total CPU time	14.37 h	19.42 h

CONCLUSIONS

A set of storm surge simulations were conducted with the model ADCIRC+SWAN, using existing model grids and high-resolution lidar surveys, to illustrate the current vulnerability of the Staten Island ocean-facing coast to extreme storms. The simulations indicate that the storm surge reduction from the "as built" protective dunes on the Staten Island southeast coastline is significantly different than the "as designed" model of the NYCDPR dune.

The resolution of the unstructured grid, which influences how well hydraulic features are represented, is an important factor in modeling the storm surges in areas where the land surface characteristics and topography vary, such as where beaches grade into dune systems. Small differences in topography that can affect storm surge inundation levels can be detected using high-resolution lidar and provide substantial guidance in implementing these important features in model grids. Therefore, the high-resolution grid representation is essential for capturing the effects of topographic features.

The computer time required for the fine grid model is approximately 20 h using 256 cores on a Cray XE6M; however, the wall clock time could involve days to a week depending on the availability of the required number of cores. If computational resources are available, simulations with finer grids and additional storm scenarios could provide effective tools for evaluating design alternatives for flood prevention structures and assessment of potential storm surge impacts on Staten Island.

Given the historical record of extreme inundation events in the New York Metropolitan area and projected increases in mean sea levels, storm surge events similar in scale to Hurricane Sandy are expected to occur in the future, with potentially greater consequences. The ADCIRC storm surge simulations based on post-Sandy fine-scale topography provide much-needed information for understanding Staten Island's changing vulnerability to storm surge inundation and for informing efforts to improve resiliency to future storms.

ACKNOWLEDGMENTS

The CUNY-IHPCC is operated by the College of Staten Island and funded, in part, by The City University of New York, New York State, New York City, the CUNY Research Foundation, and grants from the National Science Foundation grants CNS-0958379 and CNS-0855217. We are grateful to ARCADIS for providing the fine grid. We thank Terry Mares and Debbie Mahoney for assistance in preparation of the manuscript as well as Jennifer Freund for assistance with the figures. We are grateful to Paul Muzio for his computational support and review of the manuscript. We also thank four anonymous reviewers for their thoughtful comments. Any use of trade, firm, or product names is for descriptive purposes only and does not imply endorsement by the U.S. Government.

LITERATURE CITED

Atkinson, J.H.; Westerink, J.J., and Hervouet, J.M., 2004. Similarities between the wave equation and the quasi-bubble solutions to the shallow water equations. *International Journal for Numerical Methods in Fluids*, 45, 689–714.

Benimoff, A.I.; Blanton, B.O.; Dzedzits, E.; Fritz, W.J.; Kress, M.E., and Muzio, P., 2012. Storm surge model for New York, Connecticut, and northern waters of New Jersey with special emphasis on New York Harbor. *GSA Abstracts with Programs,* 44(7), 389.

Benimoff, A.I.; Fritz, W.J., and Kress, M.E., 2015. Superstorm Sandy and Staten Island: Learning from the Past, Preparing for the Future. *In*: Bennington, J.B and Farmer, E.C. (eds.), *Learning from the Impact of Superstorm Sandy*. Amsterdam: Elsevier, pp. 21–40.

Bilskie, M.V. and Hagen, S.C., 2013. Topographic accuracy assessment of bare earth lidar-derived unstructured meshes. *Advances in Water Resources,* 52, 165–177.

Blanton, B.O.; Seim, H.; Luettich, R.; Lynch, D.; Werner, F.; Smith K.; Voulgaris G.; Bingham F., and Way, F., 2004. Barotropic Tides in the South Atlantic Bight. *Journal of Geophysical Research,* 109(C1204). doi:10.1029/2004JC002455.

Blanton, B.O.; McGee J.; Fleming, J.; Kaiser, C.; Kaiser, H.; Lander, H; Luettich, R.; Dresback, K., and Kolar R., 2012. Urgent computing of storm surge for North Carolina's coast, *Proceedings of the International Conference on Computational Science*, 9(0), pp. 1677–1686.

Blanton, B.O., 2008. *North Carolina Coastal Flood Analysis System: Computational System*. Chapel Hill, North Carolina: The University of North Carolina at Chapel Hill, Renaissance Computing Institute, *Technical Report TR-08-04*.

Blumberg, A. and Georgas N., 2008. Quantifying uncertainty in estuarine and coastal ocean circulation modeling. *Journal of Hydraulic Engineering*, 134(4), 403–415.

Booij, N.; Ris, R., and Holtuijsen, L., 1999. A third-generation wave model for coastal regions, part I: model description and validation. *Journal of Geophysical Research,* 104(C4), 7649–

7666.

Bouws E. and Komen, G.J., 1983. On the balance between growth and dissipation in an extreme depth-limited wind-sea in the southern North Sea. *Journal of Physical Oceanography*, 13, 1653–1658.

Bowman, M.J.; Colle B.A., and Bowman H., 2012. Storm Surge Modelling for the New York City Region. *In*: Aerts, J.; Botzen, W.; Bowman, M.; Dircke, P., and Ward, P. (eds.), *Climate Adaptation and Flood Risk in Coastal Cities*. London: Earthscan, pp. 75–92.

Brandon, C.M.; Woodruff, J.D.; Donnelly, J.P., and Sullivan, R.M., 2014. How unique was Hurricane Sandy? Sedimentary reconstructions of extreme flooding from New York Harbor. *Scientific Reports*, http://dx.doi.org/10.1038/srep07366.

Bunya, S.; Dietrich, J.C.; Westerink, J.J.; Ebersole B.A.; Smith, J.M.; Atkinson, J.H.; Jensen, R.; Resio, D.T.; Luettich, R.A.; Dawson, C.; Cardone, V.J.; Cox, A.T.; Powell, M.D.; Westerink, H.J., and Roberts, H.J., 2010. A high-resolution coupled riverine flow, tide, wind, wind wave, and storm surge model for southern Louisiana and Mississippi: Part I – model development and validation. *Monthly Weather Review,* 138, 345–377.

Coch, N.K., 1999. Hurricane hazards in New Jersey. *In*: Puffer, J. (ed.), *Geological Association of New Jersey Annual Proceedings*. Trenton, New Jersey: Geological Association of New Jersey, p. 65.

Coch, N.K., 2012. Hurricane Irene (2011) A hydrological catastrophe in the northeast U.S. *Professional Geologist*, Sept–Oct: 47–51.

Coch, N.K., 2014. Hurricane Sandy inland water damage in the NY–NJ metropolitan area: A new perspective on the nature of urban flooding in the northeast United States. *Professional Geologist*. Apr–June: 42–46.

Coch, N.K., 2015. Unique vulnerability of the New York–New Jersey Metropolitan Area to hurricane destruction. *Journal of Coastal Research*, 31(1), 196–212.

Colle, B.F.; Buonaiuto, M.; Bowman, R.; Wilson, R.; Flood, R.; Hunter, R.; Mintz, A., and Hill, D., 2008. New York City's vulnerability to coastal flooding. *Bulletin of the American Meteorological Society*, 89(6), 829–841.

Dietrich, J.C.; Zijlema M.; Westerink, J.J.; Holthuijsen, L.; Dawson, C.; Luettich, R.A.; Jensen R.E.; Smith J.M.; Stelling, G.S., and Stone, G.W., 2011. Modeling hurricane waves and storm surge using integrally coupled, scalable computations. *Coastal Engineering*, 58, 45–65.

Egbert, G. and Erofeeva, S., 2002. Efficient inverse modeling of barotropic ocean tides. *Journal of Atmospheric and Oceanic Technology*, 19(2), 183–204.

Elsener, J.B. and Kara, A.B., 1999. *Hurricanes of the North Atlantic*. New York: Oxford University Press, 488p.

Ferreira C.M.; Olivera F., and Irish J.L., 2014. Arc StormSurge: Integrating hurricane storm surge modeling and GIS. *Journal of the American Water Resources Association,* 50(1) 219–233.

Fleming, F.; Fulcher, C.; Luettich, R.; Estrade, B.; Allen, G., and Winer, H., 2008. A Real Time Storm Surge Forecasting System Using ADCIRC. *In*: Spaulding, M. (ed.), *Estuarine and Coastal Modeling X.* Reston, Virginia: American Society of Civil Engineers, pp. 373–392.

Forbes, C.; Rhome, J.; Mattocks, C., and Taylor, A., 2014. Predicting the storm surge threat of Hurricane Sandy with the National Weather Service SLOSH Model. *Marine Science and Engineering*, 2, 437–476.

Hall, T.M. and Sobel, A.H., 2013. On the impact angle of Hurricane Sandy's New Jersey landfall. *Geophysical Research Letters*, 40, 2312–2315.

Jelesnianski, C.; Chen, J., and Shaffer, S., 1992. SLOSH: Sea, lake, and overland surges from hurricanes. *Technical Report NOAA Tech. Rep. NWS 48, NOAA/AOML Library*, Miami, FL.

Jin, S.; Yang, L.; Danielson, P.; Homer, C.; Fry, J., and Xian, G., 2013. A comprehensive change detection method for updating the National Land Cover Database to circa 2011. *Remote Sensing of Environment*, 132, 159–175.

Lin, N.; Emanuel, K.; Smith, J., and Vanmarcke, E., 2010. Risk assessment of hurricane storm surge for New York City. *Journal Geophysical Research*, 115(D18121).

Luettich, R.A.; Westerink, J.J., and Scheffner, N.W.,1992. *ADCIRC: An Advanced Three-Dimensional Circulation Model for Shelves, Coasts, and Estuaries. Report 1. Theory and Methodology of ADCIRC-2DDI and ADCIRC-3DL*. Vicksburg, Mississippi: United States Army Engineers Waterways Experiment Station, *Dredging Research Program Technical Report*, DRP-92-6, 156p.

Mattocks, C. and Forbes, C., 2008. A real-time, event-triggered storm surge forecasting system for the state of North Carolina. *Ocean Modelling*, 25(3–4), 95–119.

McCallum, B.E.; Wicklein, S.M.; Reiser, R.G.; Busciolano, R.; Morrison, J.; Verdi, R.J.; Painter, J.A.; Frantz, E.R., and Gotvald A.J., 2012. *Monitoring Storm Tide and Flooding from Hurricane Sandy along the Atlantic coast of the United States, October 2012. USGS Open-File Report 2013-1043,* 42p.

Niedoroda, A.; Resio, D.; Toro, G.; Divoky, D.; Das, H., and Reed C., 2010. Analysis of the coastal Mississippi storm surge hazard. *Ocean Engineering,* 37(1), 82–90.

NOAA (National Oceanic and Atmospheric Administration), 2013. National Hurricane Center Data Archive. http://www.nhc.noaa.gov/data/#hurdat.

Orton, P.; Georgas, N.; Blumberg, A., and Pullen, J., 2012. Detailed modeling of recent severe storm tides in estuaries of the New York City region. *Journal of Geophysical Research: Oceans*, 117(C9).

Pilkey, O.H.; Neal, W.J.; Kelley, J.T., and Cooper, A.G., 2011. *The World's Beaches*. Berkeley, California: University of California Press, 283p.

PlaNYC, 2013. A Stronger More Resilient New York. http://smedia.nyc.gov/agencies/sirr/SIRR_spreads_Hi_Res.pdf.

Qi, J.; Chen, C.; Beardsley, R.; Perrie, W., and Cowles, G., 2009. An unstructured-grid finite-volume surface wave model (FVCOM-SWAVE): Implementation, validations and applications. *Ocean Modelling*, 28, 153–166.

Roelvink, D.; Reniers, A.; van Dongeren, A.; van Thiel de Vries; J.; McCall, R., and Lescinski, J., 2009. Modelling storm impacts on beaches dunes and barrier islands. *Coastal Engineering*, 56(11–12), 1133–1152.

Scileppi, E. and Donnelly, J.P., 2007. Sedimentary evidence of hurricane strikes in western Long Island New York. *Geochemistry, Geophysics, Geosystems*, 8 (Q06011). doi:10.1029/2006GC001463.

Simonson, A.E. and Behrins, R. 2015. Measuring Storm Tide High-water Marks Caused by Hurricane Sandy in New York. *In:* Bennington, J.B. and Farmer, C.E. (eds.), *Learning from the Impact of Superstorm Sandy.* Amsterdam: Elsevier, pp. 7–19.

Sweet, W.; Zervas, C.; Gill, S., and Park, J., 2013. Hurricane Sandy inundation probabilities today and tomorrow. *Bulletin of the American Meteorological Society*, 94, S17–S20.

Talke, S.A.; Orton, P., and Jay, D.A., 2014. Increasing storm tides in New York Harbor, 1844–2013. *Geophysical Research Letters*, 41(9), 3149–3155.

USACE (United States Army Corps of Engineers), 2012. Joint Airborne Lidar Bathymetry Technical Center of Expertise, Topobathy Lidar: Post Super Storm Sandy - Coastal New Jersey and New York. http://www.csc.noaa.gov/dataviewer/index.html?action=advsearch&qType=in&qFld=ID&qVal=2478.

USGS (United States Geological Survey), 2012. Sandy mapper database. http://water.usgs.gov/floods/events/2012/sandy/sandymapper.html.

Vledder, G.; Zijlema, M., and Holthuijsen, L., 2011. Revisiting the JONSWAP bottom friction formulation. *Coastal Engineering Proceedings,* 1(32), 41. doi:http://dx.doi.org/10.9753/icce.v32.waves.41.

Wamsley, T.; Cialone, M.; Smith, J.; Atkinson J., and Rosati, J., 2010. The potential of wetlands in reducing storm surge, *Ocean Engineering*, 37, 59–68.

Wang, H.V.; Loftis, J.D.; Liu, Z.; Forrest, D., and Zhang, J., 2014. The storm surge and sub-grid inundation modeling in New York City during Hurricane Sandy. *Journal of Marine Science and Engineering*, 2, 226–246.

Westerink, J.; Luettich, R., and Muccino, J., 1994. Modeling tides in the western North Atlantic using unstructured graded grids. *Tellus,* 46a, 125–152.

Westerink, J.; Luettich, R.; Feyen, J.; Atkinson, J.; Dawson, C.; Roberts, H.; Powell, M.; Dunion, J.; Kubatko, E., and Pourtaheri, H., 2008. A basin- to channel-scale unstructured grid hurricane storm surge model applied to southern Louisiana. *Monthly Weather Review*, 136, 833–864.

Zhang, Y. and Baptista, A.M., 2008. SELFE: A semi-implicit Eulerian-Lagrangian finite-element model for cross-scale ocean circulation. *Ocean Modelling*, 21(3–4), 71–96.

Zijlema, M., 2010. Computation of wind-wave spectra in coastal waters with SWAN on unstructured grids. *Coastal Engineering,* 57(3), 267–277.